

ULTIMATE CAPACITY PREDICTION OF CARBON FIBER REINFORCED POLYMERS (CFRP) STRENGTHENED REINFORCED CONCRETE FLEXURAL ELEMENTS BASED ON DEBONDING FAILURE

B.C.R Jayanath,
University of Moratuwa Sri Lanka
rajeevjayanath@gmail.com
Dr. C. S. Lewangamage,
University of Moratuwa Sri Lanka
sujeewal@uom.lk
Prof. M. T. R. Jayasinghe,
University of Moratuwa Sri Lanka
thishan@uom.lk
N. Prakash,
University of Moratuwa Sri Lanka
prakashn3@gmail.com

Abstract

The ultimate strength of reinforced concrete elements retrofitted in flexure by means of externally bonded carbon fiber reinforced polymers (CFRP) has attracted the attention of researchers due to many advantages highlighted by a wide set of experimental results. The current paper presents analytical and experimental study on reinforced concrete (RC) flexural elements strengthened for flexure with externally bonded CFRP. A simple yet rational model is developed, based on cross sectional analysis, satisfying strain compatibility and equilibrium conditions, which is capable of predicting the ultimate moment capacity of (Fiber Reinforced Polymers) FRP strengthened flexural sections. A total number of nine specimens, including three beams, and six numbers of one way spanning slabs were cast. One beam and three slabs were kept as control specimens having no strengthening with CFRP and the other specimens were strengthened with CFRP laminates and tested under the “four point loading arrangement”. Debonding strain at the ultimate failure is calculated based on the experimental results and compared with the existing design standards. The test results indicated that significant enhancement of load carrying capacity can be achieved by externally reinforced with CFRP.

Keywords: FRP, debonding, flexure, strain

1. Introduction

Strengthening reinforced concrete (RC) structures with FRP composites is becoming an attractive alternative for the construction industry and rehabilitation of existing concrete structures. In particular, flexural and shear FRP reinforcing elements, externally bonded to reinforced concrete (RC) elements constitute a larger body of the actual applications.

Reinforced concrete (RC) slabs and beams would generally fail in flexure. However, many RC structures could encounter shear and flexural problems due to various reasons such as mistakes in design calculations, improper detailing of reinforcements, poor construction practices, changing the function of a structure from lower service load to a higher service load and reduction in or total loss of reinforcement steel area causing corrosion in service environments etc. [1].

For strengthening shear deficient structural elements, as well as flexural strengthening, numerous tests have been carried out [2-5] and shown that composite materials would be an excellent option for external reinforcing. Rehabilitation of these structures can be in the form of strengthening of structural members, repair of damaged structures or retrofitting for seismic deficiencies. In any case, composite materials are an excellent option to be used as external reinforcing because of their high tensile strength, light weight, resistance to corrosion and ease of installation. Externally bonded FRP reinforcements have been shown to be applicable for the strengthening of many types of RC structures such as columns, beams, slabs, walls, tunnels, chimneys and silos. FRP can be used not only to improve flexural capacity but also provides confinement and ductility to structural members.

Number of research studies have been carried out in the recent past, to investigate the effects of various parameters on the behavior of FRP strengthened beams and slabs in flexure [6, 7]. The ultimate load of the strengthened RC flexural member depends principally on the compressive strength of the concrete, the yield strength of shear and longitudinal reinforcement, the tensile reinforcement ratio, span to depth ratio, the composite materials strength ratio, etc. Therefore, in past research attention has been placed on performance and failure modes of FRP strengthened flexural elements that were strengthened by using different arrangements and widths of CFRP straps [8]. In case of flexural strengthening, bonding of CFRP at the bottom of the tension side of the flexural element is preferred. In this way, the internal couple is increased, without increasing the weight of the structure.

Experimental studies have shown that strengthened beams generally fail prematurely in a brittle and sudden manner due to debonding between FRP and concrete substrate. Hence, the full strength of the strengthening area cannot be utilized [9-11].

Based on the possible failure modes, analytical studies have been carried out to predict the ultimate capacity of the beams. The parametric analysis conducted by An W et al [12] shows the effect of design variables, such as external plate area, concrete compressive strength, plate stiffness and strength and internal reinforcement ratio. It is generally assumed that the gain in

strength and stiffness are usually associated with a decrement in ductile behavior of the structure. But it is evident that the FRP strengthened beams have shown more ductile behavior than the RC beams and slabs.

Various analytical models have been proposed to predict the behavior of FRP strengthened systems. Some analytical models that predict the behavior of FRP strengthened beams [13-15] were based on iterative techniques, assuming that the beam fails in fully composite flexural failures by either concrete crushing or rupture of the FRP laminates.

Tarek H. Almusallam and Al-Salloum [16] developed a model to predict the ultimate capacity of FRP strengthened beams considering the balanced laminate thickness, i.e.: assuming that the additional forces are balanced by the FRP laminates and maintain the static equilibrium at the ultimate state.

Since the debonding failure is the most unpredictable failure mode of the FRP strengthened structures, the criterion should be addressed with a care. The adhesion between the FRP sheet and the concrete substrate is the most critical factor for the debonding. The design standards follow various approaches to encounter FRP debonding failure. Practice of strength predictions recommended by Canadian Standards Association suggested that the maximum allowable strain in the FRP composite to be limited to 50% of the rupture strain. ACI-440-2R-08 [17], Japanese standards [18] and ECP 208-2005 [19] also limit the FRP strain to certain amount to encounter the debonding failure.

The current paper evaluate the performance, effectiveness and the modes of failure of beams, one way spanning RC slabs strengthened with CFRP under flexure and to verify existing debonding models for different types of strengthening schemes. A simple and efficient computational analysis model is presented to predict the ultimate capacity of FRP strengthened beams and slabs.

2. Experimental study

2.1 Flexural strengthening of slabs

2.1.1 Specimen details

Three slabs (125 mm × 500 mm × 1530 mm) were singly reinforced at tension side by four numbers of 6 mm mild steel bars (250 N/mm²) and the other two slabs were singly reinforced at tension side by three numbers of 10 mm tor steel bars (460 N/mm²) with a concrete clear cover of 25 mm. This corresponds to a steel reinforcement ratio of about 0.18% and 0.38%. For the strengthened slabs, Carbon Fiber Reinforced Polymer (CFRP) strips having a width of 200 mm and a thickness of 1 mm was bonded to the tension face of the slab with two different

arrangements, which corresponded to a CFRP reinforcement ratio of about 0.32% and 0.64%. The slabs identifications and the details are shown in Table 1 and cross sectional details are shown in Figures 1 to 6.

Table 1: Specimen details of slabs

Slab	Dimension (mm)			r/f details
	height	width	length	
Control Specimen- R6-CS1 & R6-CS2	125	500	1530	4 R6 @ 150mm
FRP bonded specimen- R6-TS1	125	500	1530	4 R6 @ 150mm
FRP bonded specimen- R6-TS2	125	500	1530	4 R6 @ 150mm
Control Specimen- T10-CS	125	500	1530	3 T10 @ 225mm
FRP bonded specimen- T10-TS1	125	500	1530	3 T10 @ 225mm

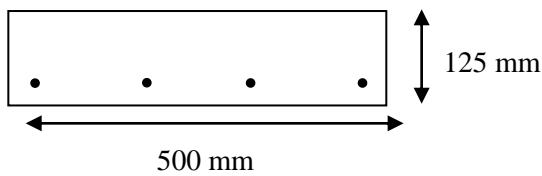


Figure 1: R6CS

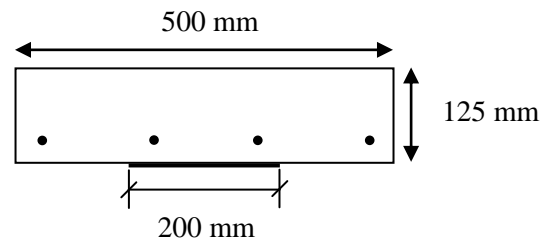


Figure 2: R6TS1 one layer TYFO SCH41 Carbon Strip 200mm wide.

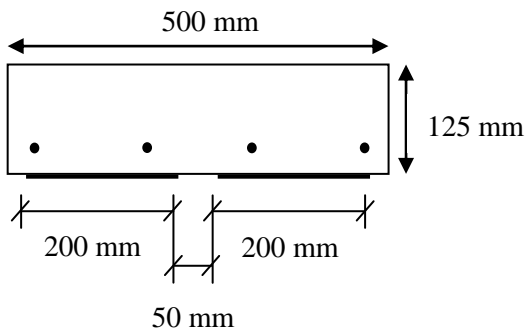


Figure 3: R6TS2 two layer TYFO SCH41 Carbon Strips 200mm wide each

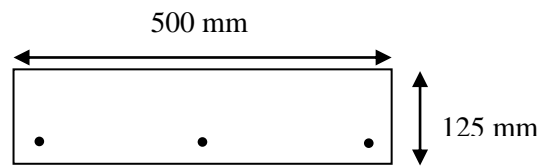


Figure 4: T10CS1

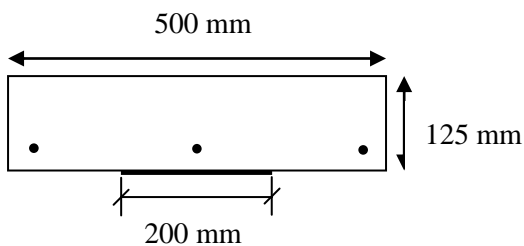


Figure 5: T10TS1 one layer TYFO SCH41 Carbon Strip 200mm wide

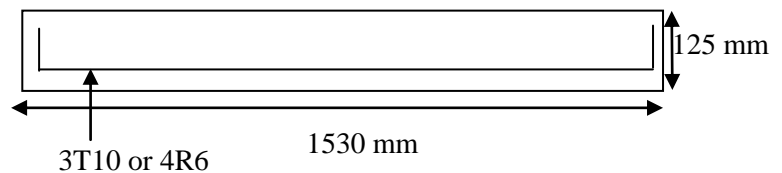


Figure 6: longitudinal section of the slabs

Table 2:properties of FRP and composite

Typical dry fiber properties	
Tensile Strength	3.79 GPa
Tensile Modulus	230GPa
Ultimate Elongation	1.7%
Density	1.74 g/cm ³
Weight per sq.meter	644 g/m ²
Composite gross laminate properties	
Ultimate tensile strength	834MPa
Elongation at break	0.85%
Tensile Modulus	82GPa
Laminate thickness	1.00 mm

2.1.2 Testing procedure of slabs

The slabs were tested in four point bending, being simply supported on a pivot bearing on either side over a span of 1350 mm. Identical bearing pads were placed at the loading points on top of the beams. A spreader plate resting on top of these provided a system for load distribution. Load was applied monotonically at the mid-span of the slab using a hydraulic jack and a loading (proving) ring having a capacity of 100 kN. Load was applied by the increment of 5kN for the control specimens and with the increment of 10kN for other three testing specimens. Deflection of the slabs was noted at each load increment and the crack development was observed. Figure 7 shows a schematic diagram of a typical test specimen with loading arrangement.

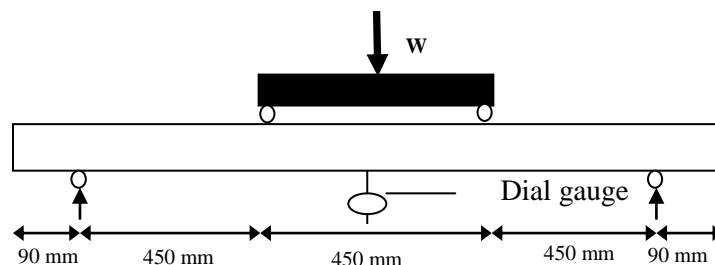


Figure 7: Loading arrangement of slabs

2.2 Flexural strengthening of beams

2.2.1 Specimen details

Three beams having length of 2000 mm, with 200 mm × 150 mm cross section, were cast. One beam was kept as control specimen and the other two were strengthened with CFRP. Cross sections of the control beam and CFRP strengthened beams with the reinforcement details are given in Figures 8 and 9. Grade 30 concrete was used for the beams and the properties of CFRP composites are same as given in Table 2.

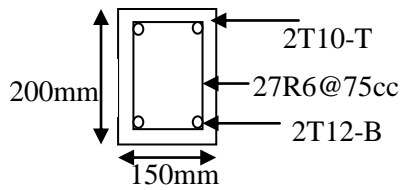


Figure 8: Cross section of a beam

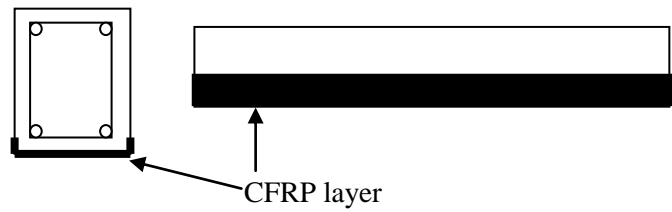


Figure 9: CFRP arrangement of the beams

2.2.2 Testing procedure of beams

The beams were tested in four point bending, being simply supported on a pivot bearing on either side over a span of 1800 mm. Identical bearing pads were placed at the loading points on top of the beams. A spreader I-beam resting on top of these provided a system for load distribution. Load was applied by increments of 5kN throughout the tests. Deflections were measured at the center. The loading arrangement and the dial gauge position are shown in Figure 10. At each load increment, locations of crack development on the concrete beams were also noted.

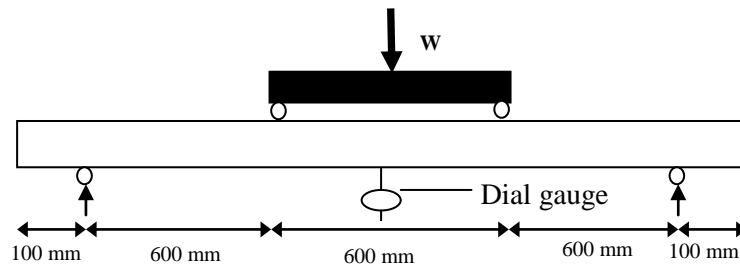


Figure 10: Loading arrangement of beams

3. Flexural capacity

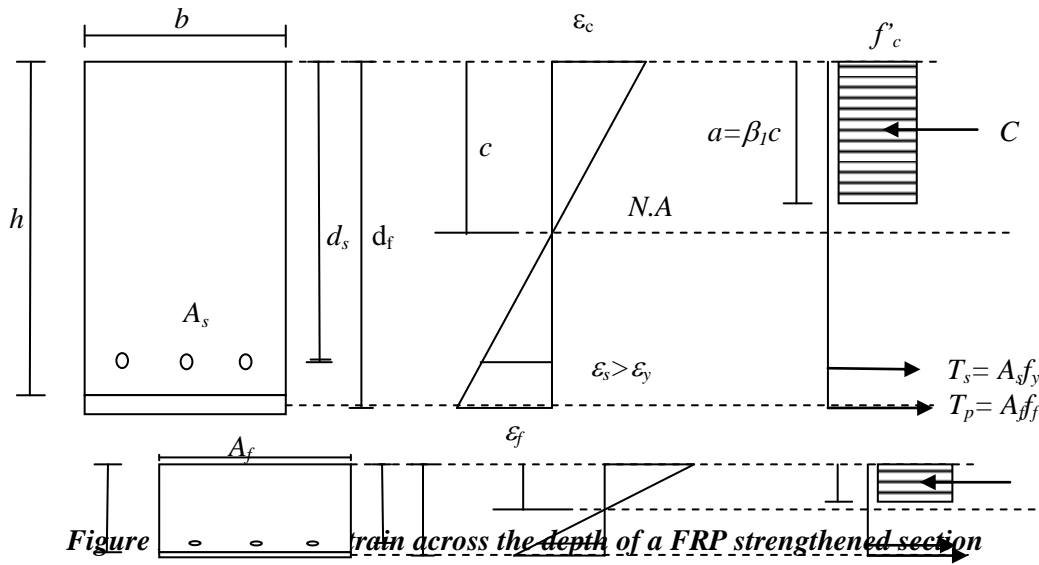
The experimental studies conducted on RC beams strengthened in flexure with FRP wraps, encountered in three major failure modes: (i) classical failure of the beam. (ii) tension failure of FRP laminate and (iii) the premature debonding failure. The classical failure corresponds to either crushing of concrete in compression or tension failure in the steel after yielding. Tension failure can be achieved when the FRP laminate reaches its ultimate strength. The debonding failure occurs due to bond failure between FRP and concrete substrate.

The ultimate capacity prediction is based on a section analysis (Figure 11) The ultimate moment capacity, M_u can be determined by taking the moment about the line in which the concrete compression force acts and can be expressed as

$$M_u = A_s f_y \left(d - \frac{a}{2} \right) + A_f f_f \left(d_f - \frac{a}{2} \right) \quad (1)$$

Where $a = \beta_1 c$ and $f_f = E_f \varepsilon_f$ in which

d_s = distance from the extreme compression fiber to the centroid of tension reinforcement
 d_f = distance from the extreme compression fiber to the centroid of FRP reinforcement
 A_s = area of tension steel reinforcement
 A_p = area of FRP laminate
 β_f = ratio of rectangular compression block to the depth of neutral axis
 f_y = yield stress of steel reinforcement
 f_f = the tensile stress in the FRP laminate
 f_{fu} = the ultimate tensile stress in the FRP laminate
 E_f = modulus of elasticity of FRP laminate
 ε_f = the strain in the FRP laminate, corresponding to f_f
 ε_{fd} = debonding strain of FRP



The ultimate moment of the section can be determined by an iterative procedure. According to FRP strain at failure, concrete strain ε_c , and steel strain ε_s , are determined using equations 2 and 3.

When debonding occurs, FRP strain at failure $\varepsilon_f = \varepsilon_{fd}$

$$\varepsilon_c = \frac{c\varepsilon_f}{(d_f - c)} \quad (2)$$

$$\varepsilon_s = \frac{\varepsilon_f(d_s - c)}{(d_f - c)} \quad (3)$$

Based on the strain values, the compressive force in concrete (C), tensile force in FRP laminates (T_p) and tensile force in steel (T_s) can be calculated and the static equilibrium is verified by adjusting the value of a .

Steel stress at failure f_s , and stress in the FRP laminates f_f can be expressed in terms of strains (equations 4 and 5).

$$f_s = \varepsilon_s E_s \leq f_y \quad (4)$$

$$f_f = \varepsilon_f E_f \quad (5)$$

Ratio of the rectangular compression block to the depth of neutral axis β_1 is calculated from equation 6, which given in ACI 318M-08[20].

$$\beta_1 = 1.05 - \frac{0.05f'_c}{6.9} \quad (6)$$

The existing debonding criteria for the calculation are listed below.

ACI 440.2R-08:

$$\varepsilon_{fd} = 0.41 \sqrt{\frac{f'_c}{nE_f t_f}} \leq 0.9f_{fu}$$

$$f_{fu} = C_E \varepsilon_{fu}^*$$

Where, C_E is the environmental reduction factor which can be taken as 0.95, ε_{fu}^* is the ultimate strain of FRP, ε_{fd} is the debonding strain of FRP, f'_c is the concrete compressive strength, n is the number of FRP plies, E_f is the modulus of elasticity of FRP material and t_f is the thickness of the FRP layer.

The Egyptian code ECP 208-2005:

$$\varepsilon_{fe} = k_m \varepsilon_{fu}$$

$$k_m = \begin{cases} \frac{1}{60 \varepsilon_{fu}} \left(1 - \frac{nE_f t_f}{360000} \right) \leq 0.9 \text{ for } nE_f t_f \leq 180000 \\ \frac{1}{60 \varepsilon_{fu}} \left(\frac{90000}{nE_f t_f} \right) \leq 0.9 \text{ for } nE_f t_f > 180000 \end{cases}$$

Where, ε_{fe} is the effective FRP strain, n is the number of plies, E_f is the modulus of elasticity of FRP material and t_f is the thickness of the FRP layer.

Japanese standard

$$\varepsilon_{fd} = \sqrt{\frac{2G_f}{n_f E_f t_f}}$$

Where G_f is the interfacial fracture energy between FRP and concrete and its value can be taken as 0.5 N/mm².

4. Results and validation

4.1 Slabs

Data gathered from experimental programme are summarized in table 3, in terms of failure load and the failure mode.

Table 3: Failure loads and failure modes of beams.

Slab		Failure load (kN)	Failure mode
Control Specimens	R6-CS1	18.24	Concrete crushing
	R6-CS2	18.21	
FRP bonded specimen-R6-TS1		48.56	CFRP debonding
FRP bonded specimen-R6-TS2		85.61	CFRP debonding
Control Specimen-T10-CS		29.17	Concrete crushing
FRP bonded specimen-T10-TS1		82.16	CFRP debonding

Control specimens were failed in steel yielding and concrete crushing. Flexural cracks were observed during the failure (Figures 12 and 13).



Figure 12: Crack propagation of R6-CS1

Figure 13: Crack propagation T10-CS1

The FRP strengthened slabs were failed in FRP debonding and concrete crushing, resulting a brittle type failure. The FRP laminates were separated from the concrete surface without rupture, (Figure 14)



Figure 14: Debonding failure of FRP strengthened slabs

Load vs. deflection relationships of the specimens are shown in figures 10 and 11.

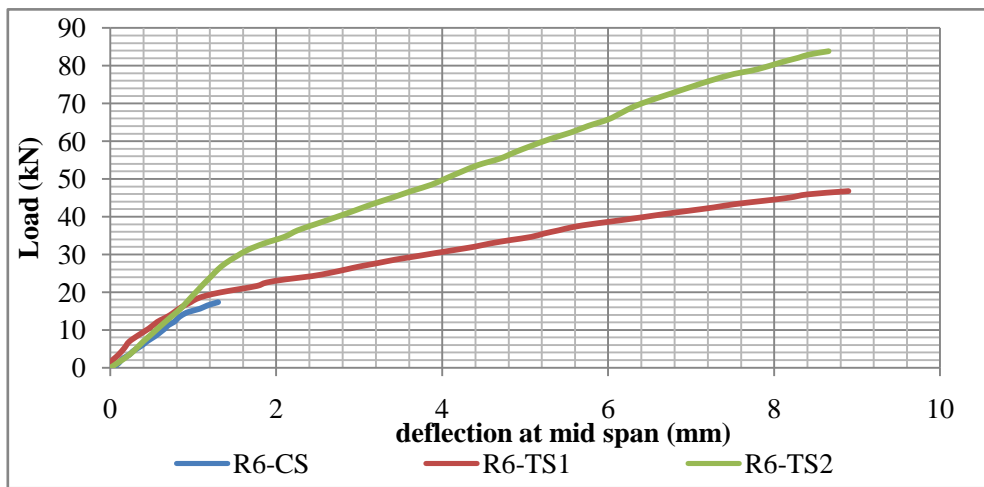


Figure 15: Load Vs Deflection curve of the mid span of the slabs for R6CS, R6TS1 and R6TS2

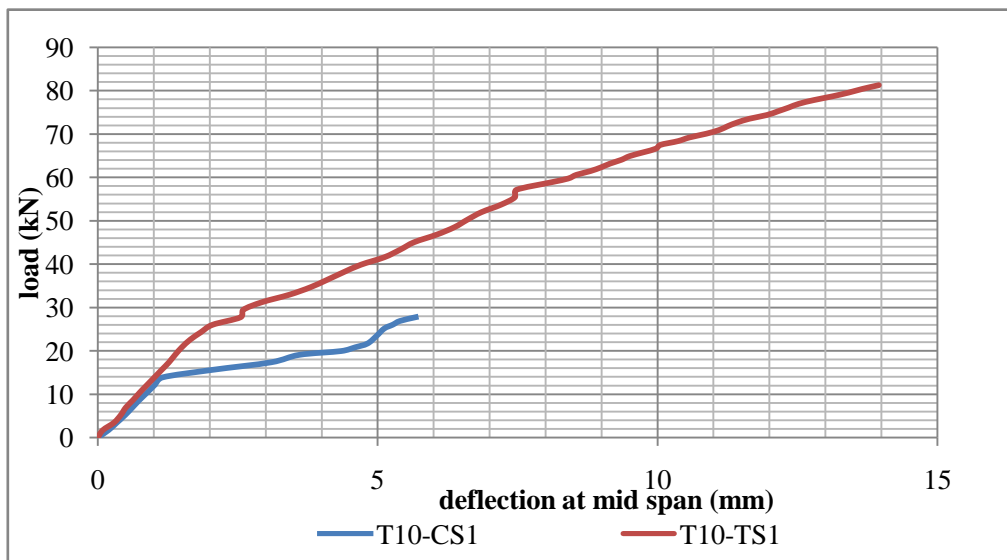


Figure 16: Load Vs Deflection curve of the mid span of the slabs for T10CS1 and T10TS1

It was observed that nearly 150 % strength increment could be achieved in this particular case.

The predicted moment capacities by using the values of debonding strain, proposed by the guidelines and the experimental moment capacities of the slabs are compared in Table 4.

Table 4 Comparison of predicted ultimate moment capacities with experimental values

Specimen	Predicted ultimate moment capacity (kNm)			Experimentally (kNm)
	ACI 440-2R-08	Japanese standards	Egyptian code ECP 208-	
R6TS1	17.25	9.80	17.99	10.92
R6TS2	31.01	16.69	32.42	19.26
T10TS1	24.56	17.24	25.29	18.48

4.2 Beams

Data gathered from experimental programme are summarized in table 5, in terms of failure load and the failure mode. Summary of the failure loads and the failure modes are given in Table 5.

Table 5: Comparison of failure loads in beams

Beam	Experimental Failure load (kN)	Failure mode
Control Specimen	66	Concrete crushing
CFRP bonded specimen-01(TB1)	120	Concrete crushing and CFRP debonding
CFRP bonded specimen-02(TB2)	123	CFRP debonding

Figure 17 shows the flexural cracks propagation on the control specimen and Figure 18 shows the failure mode of the CFRP bonded specimens.



Figure 17: Flexural cracks in control beam



Figure 18: Debonding failure of FRP strengthened beam

Deflection pattern of the CFRP strengthened beams were almost the same and failure load was doubled compare to the control specimen. Figure 19 shows the Load Vs. Deflection of the mid span.

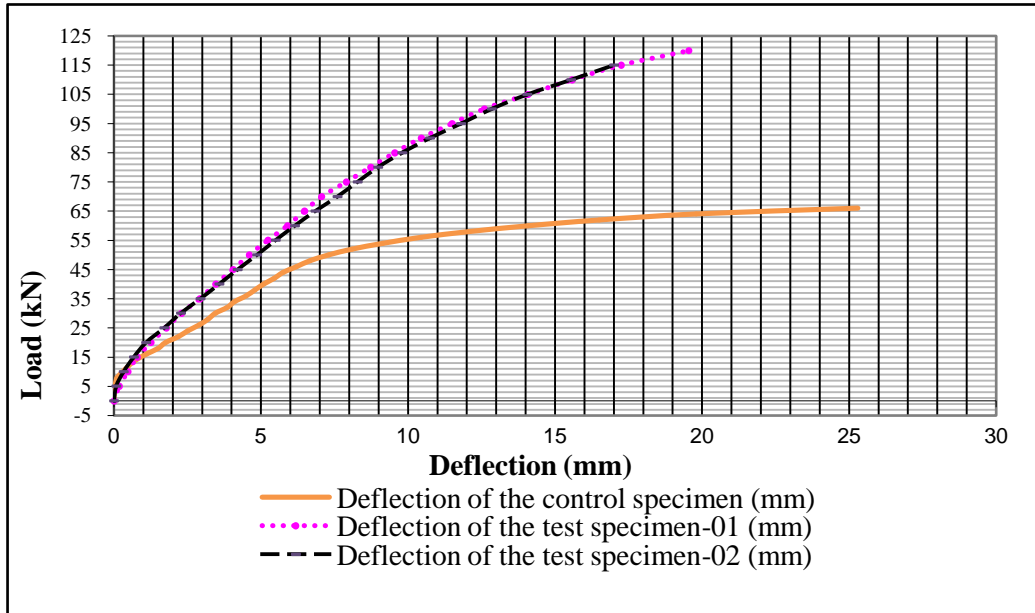


Figure 19: Load Vs deflection curve of the mid span of the beams

It was observed that nearly 84% strength increment could be achieved in this particular case.

The predicted moment capacities by using the values of debonding strain, proposed by the guidelines and the experimental moment capacities of the beams are compared in table 6.

Table 6: Comparison of predicted ultimate moment capacities with experimental values

Specimen	Predicted ultimate moment capacity (kNm)			Experimentally(kNm)
	ACI 440-2R-08	Japanese standards	Egyptian code ECP 208-	
TB1	38.83	28.15	39.87	36.00
TB2	38.83	28.15	39.87	36.90

Table 7 summarizes the debonding strains which were calculated by using, ACI 440-2R-08, Japanese standards, Egyptian standards and compared with the strain values calculated based on the experimental results.

Table 7: Comparison of debonding strain values

Specimen	Debonding strain at ultimate failure			
	From experiment	ACI 440-2R-08	Japanese standards	Egyptian code ECP 208-2005
R6TS1	0.00415	0.00727	0.00349	0.00765
R6TS2	0.00415	0.00727	0.00349	0.00765
T10TS1	0.00415	0.00727	0.00349	0.00765
TB1	0.00625	0.00726	0.00349	0.00765
TB2	0.00625	0.00726	0.00349	0.00765

The bonding stresses of CFRP-concrete interface are mainly shear and normal stresses. CFRP on bottom of the beams and the slabs, which are used for flexural strengthening, carries tensile stresses transferred through interface shear stresses and improves the bending load carrying capacity of the structural elements. The interface bonding also has influence on strengthened flexural behavior. At the end part of CFRP where there is a truncation of FRP, stress concentrations occurred which leads to the CFRP de-bonding.

As predicted by the existing guide lines, debonding strain at the failure was calculated and compared with the debonding strain values calculated by using the experimental results. The comparison of the results given in Table 7 show that the variation of the results.

5. Conclusion

The structural performance of RC beams and slabs strengthened with CFRP sheets has been evaluated. The flexural tests carried out in this study demonstrated that external bonding of CFRP sheets is an effective technique of strengthening. The experimental results showed that the CFRP bonded with epoxy could effectively improve the structural performance of RC beams by increasing both the load carrying capacity and the corresponding ductility compared with unstrengthened RC beams.

The experimental results show that the actual debonding strain at failure cannot be predicted according to existing guidelines. Hence, further experimental and theoretical studies will be carried out to identify and understand the complete behaviour of CFRP strengthened flexural elements under tropical climatic conditions.

Acknowledgment

This research is supported by University of Moratuwa Senate Research Grant (Grant no SRC/LT/2011/26). The authors are grateful to Mr. Dhammika Wimalaratne who provided the FRP materials for the research.

References

1. GangaRao, H. V. S., Taly, N., & Vijay, P. V., "*reinforced concrete design with FRP composites*", CRC press.
2. GangaRao, H. V. S., Faza, F. S., & Vijay, P. V., "Behavior of concrete beams wrapped with Carbon Tow sheets", *CFC report, submitted to Tonen Corporation, Tokyo*, pp. 95-196, April 1995.
3. Varastehpour, H., & Hamelin, P., "Strengthening of concrete beams using fiber-reinforced plastics", *Journal of Materials and Structures/Matériaux et Constructions*, Vol. 30, April 1997, pp 160-166. www.sciencedirect.com. [Accessed September, 2009]
4. Mays, G. C., & Barnes, R. A., "*The shear strengthening of reinforced concrete beams using bonded external reinforcement*", www.sciencedirect.com. [Accessed September, 2009]
5. Irwin, R. & Rahman, A., "*frp strengthening of concrete structures – design constraints and practical effects on construction detailing*", www.sciencedirect.com. [Accessed September, 2009]
6. Tamer E. M and Khaled S. "*Strengthening of reinforced concrete slabs with mechanically-anchored unbonded FRP system*", *Construction and Building Materials*, vol. 22, no. 4, pp. 444-455
7. Khalid M. M and Ayman S. M (2003) "*Strengthening of two-way concrete slabs with FRP composite laminates*", *Construction and Building Materials*, vol. 17, pp. 43-54
8. Lu X. Z, Ye L. P, Teng J. G, Huang Y. L, Tan Z, Zhang Z. X, "*Recent research on interfacial behavior of FRP sheets externally bonded to RC structures*". *Proceedings of the 2nd international conference on FRP composites in civil engineering*. Berlin: Springer; 2004. p. 389–98.
9. Almakht M, Bal'azs G, Pilakoutas K. "*Strengthening of RC elements by CFRP plates. Local failure*", 2do. In: Int. Ph.D. symposium in civil engineering; 1998.
10. Rosenboom O, Rizkalla S. "*Experimental study of intermediate crack debonding in fiber reinforced polymer strengthened beams*". *ACI Struct J* 2008;105(1):41–50.
11. Al-Zaid RZ, Shuraim AB, El-Sayed AK, Al-Negheimish AI, Al-Huzaimy AM. "*Flexural strengthening of shallow reinforced concrete beams using CFRP plates. 2nd international structural specialty conference*". CSCE, Winnipeg, Canada; June 9–12, 2010.
12. An W, Saadatmanesh H, Eshani M. "*RC beams strengthened with FRP plates, II: analysis and parametric study*". *J Struct Eng ASCE* 1991;117(11):3434–54.
13. Pesic N, Pilakoutas K. "*Flexural analysis and design of reinforced concrete beams with externally bonded FRP reinforcement*". *Mater Struct* 2005;38:183–92.

14. Wang Y, Chen C. “Analytical study on reinforced concrete beams strengthened for flexure and shear with composite plates”. *Compos Struct* 2003;59:137–48.
15. Ramana V, Kant T, Morton S, Dutta P, Mukherjee, Desai Y. “Behavior of CFRP strengthened reinforced concrete beams with varying degrees of strengthening”. *Compos Part B* 2000; 31:461–70.
16. Tarek H. Almusallam, Yousef A. Al-Salloum, “Ultimate strength prediction for RC beams externally strengthened by composite materials”, *Composites, Part B 32:Engineering*, pp 609-619.
17. ACI 440.2R-08. “Guide for the design and construction of externally bonded FRP systems for strengthening concrete structures.” American Concrete Institute; 2008.
18. JSCE. “Recommendations for upgrading of concrete structures with use of continuous fiber sheets.” Japan Society for Civil Engineers, Japan; 1997.
19. ECP-208-2005. “Egyptian code of practice for the use of fiber reinforced polymer (FRP) in the construction fields”. Egyptian standing code committee for the use of fiber reinforced polymer (FRP) in the construction fields 2005
20. ACI 318M-08. “Building code requirements for structural concrete (ACI 318M-08) and commentary”. American Concrete Institute; 2008.